Gait & Posture 33 (2011) 532–537

Contents lists available at ScienceDirect

Gait & Posture

journal homepage: www.elsevier.com/locate/gaitpost

A markerless estimation of the ankle–foot complex 2D kinematics during stance

Elif Surer [a,b,*], Andrea Cereatti [a,c], Enrico Grosso [b], Ugo Della Croce [a]

[a] Biomedical Sciences Department, University of Sassari, Sassari, Italy
[b] Computer Vision Laboratory, University of Sassari, Sassari, Italy
[c] Centro di Cura e Riabilitazione Santa Maria Bambina, Oristano, Italy

ARTICLE INFO

Article history:
Received 9 April 2010
Received in revised form 4 November 2010
Accepted 6 January 2011

Keywords:
Markerless
Human movement analysis
2D joint kinematics
Ankle–foot complex

ABSTRACT

A markerless technique is proposed and applied to estimate the two-dimensional joint kinematics of the shank and foot complex during the stance phase. Image sequences were acquired with a single camera from three healthy subjects while walking barefoot and with socks. Automatic segmentation of the shank and foot was performed to isolate the moving body from the background. A multi-rigid body model for the shank and foot complex, with the relevant segment anatomical axes, was defined and an image cross-correlation technique was applied to detect the anatomical axes locations throughout the movement. The proposed markerless technique was validated by acquiring the same trials also with a stereophotogrammetric marker-based system and a simple marker set. Differences in the joint kinematics estimates obtained with the two techniques fall in most cases within the intra-subject variability showing that, in selected applications, the markerless technique may replace more expensive and more experimental time demanding marker-based techniques.

© 2011 Elsevier B.V. All rights reserved.

1. Introduction

Quantitative gait analysis is generally carried out by mounting retro-reflective markers on the skin of subjects and reconstructing the three-dimensional (3D) position in the laboratory space by means of stereophotogrammetric systems. The use of stereophotogrammetry requires the placement of markers on selected points of the body segments. Typically, an expert operator spends a considerable amount of time in attaching the markers. In order to do so, subjects are often asked to remove their clothing, including shirts, shoes and socks, sometimes causing feelings of uneasiness. A technique less time consuming, requiring less expertise, discomfort-free to the subject would be favorably accepted in clinical applications.

Markerless techniques (*Ml*) have been recently presented [1] and may potentially play an important role in this respect. Different approaches have been proposed for estimating the human body kinematics based on a *Ml* approach. Corazza et al. employed a full 3D body model of the subject to be matched with the visual hull by using Simulated Annealing [2]. Bregler and Malik used twist and exponential maps to define the motion of their model [3]. Chu et al. proposed a model-free approach by describing the human body with a set of points to be mapped to a pose-invariant intrinsic space posture [4]. The use of 3D *Ml* techniques in the clinical and research fields has been so far limited due to the high computational cost [5,6] and equipment requirements [7], especially in the full body analysis.

In two-dimensional (2D) quantitative analysis of joint kinematics, *Ml* approaches could possibly be effectively implemented in clinical applications. By using a Cardboard kinematic model, Howe et al. [8] modeled the limbs as planar patches and enforced 2D constraints on capturing and analyzing the motion. To make the model representation independent of the original image, image descriptors such as silhouettes, edges, color and texture are frequently used in 2D *Ml* approaches [9]. In answering to some specific clinical questions, 3D gait analysis showed that the most significant differences between groups were concentrated in the sagittal joint kinematics [10–12], therefore, in such cases, the information provided by a 2D quantitative sagittal joint kinematics analysis may be sufficient, as long as that the main joint axis remains approximately perpendicular to the image plane throughout the recording of the motor task.

Since the shank and foot complex is key for propulsion and support during locomotion, the analysis of its kinematics provides important information for the diagnosis and treatment of pathologies affecting locomotion [13,14].

Based on the considerations above, in this study we focus to the sagittal kinematics of the shank and foot complex during the stance phase of walking, with two aims: a) to propose a 2D *Ml* technique and b) to verify if the performance of the proposed technique is affected when the subject walks with socks on (as opposed to barefoot). The proposed method was validated (both in

* Corresponding author at: Biomedical Sciences Department, University of Sassari, Viale San Pietro 43b, 07100 Sassari, Italy. Tel.: +39 079228340.
E-mail addresses: esurer@uniss.it (E. Surer), acereatti@uniss.it (A. Cereatti), grosso@uniss.it (E. Grosso), dellacroce@uniss.it (U. Della Croce).

0966-6362/$ – see front matter © 2011 Elsevier B.V. All rights reserved.
doi:10.1016/j.gaitpost.2011.01.003

barefoot and socked conditions) by acquiring the same walking trials both with a single camera (used in the *MI* approach) and a simple marker-based (*Mb*) system.

2. Materials and methods

Three healthy subjects (one male and two females; 27, 28 and 28 years old, respectively) were asked to walk at self-paced speed (approximately 0.7 m/s) in two different conditions: barefoot and wearing ankle sport socks. Five trials for each condition were recorded for each subject. All data collection was conformed to the Declaration of Helsinki on the involvement of the human subjects in biomedical research. The study was approved by the local ethical committee and subjects gave their informed consent.

The *Mb* data were acquired simultaneously with the *MI* data using a six-camera stereophotogrammetic system (Vicon MX, 1.3 Mpixel, 120 frames/s). The measurement volume was 1.5 m^3 (1.5 m × 1 m × 1 m). The markers were positioned on the head of fibula, on the calcaneus, on the lateral malleolus and on the first and fifth metatarsal heads. The marker positions were projected to 2D in the estimation of the joint kinematics. A force platform (AMTI, Watertown, MA) was also used to detect heel strikes and toe offs.

The *MI* estimate of the sagittal plane kinematics of the shank and foot complex required the execution of the following steps.

2.1. Video acquisitions

Sagittal view images of the shank and foot complex of the subjects were acquired during the stance phase with a single digital camera (Basler A101f, resolution: 800 × 600 pixels). The camera, acquiring at 15 frames/s, was positioned laterally to the subject to obtain a sagittal view of the shank and foot during the stance phase. The measurement plane was 1.5 m^2 (1.5 m × 1 m). Sample frames of acquisitions with the subject barefoot and wearing ankle socks are shown in Fig. 1a and b, respectively.

2.2. Segmentation

The objective of the segmentation procedure is to subtract the background from the moving body parts on the acquired image frames. To accomplish this aim, the Mixture of Gaussians method (MoG) [15] was applied. The MoG is a widely used statistical method, particularly effective when dealing with moving objects and illumination changes [16]. Using the combination of a finite number of Gaussian distributions rather than a single Gaussian distribution, enables the MoG method to optimally characterize the statistical content of image sub-parts, handling sequences of images with overlaps and occlusions. By calculating the variance of each Gaussian in the mixture, the correct statistical distribution of the corresponding background is determined. Pixel values that do not fit the background distributions form the foreground.

Examples of the output of the segmentation procedure are reported in Fig. 1c and d.

2.3. Multi-segment model

The multi-rigid body model adopted for the kinematic analysis consisted of three rigid body segments: shank (tibia and fibula), rearfoot (tarsus and metatarsus) and forefoot (phalanges), connected by cylindrical hinges. The model was characterized by two degrees of freedom: the ankle plantar/dorsi-flexion angle (α) and the rearfoot–forefoot flexion/extension angle (β) as described in Fig. 2a.

2.4. Anatomical axes definition

For each subject, anatomical axes were defined using a reference image (RI) extracted from the video recordings of the shank and foot complex with markers on at mid stance. In general, this phase does not require the use of markers, although it might be helpful to mark the anatomical landmarks on the subject's skin after palpation and prior to the RI acquisition. In this study, to validate the proposed *MI* technique, the same markers used for the *Mb* acquisitions were also used to identify anatomical landmarks in the RI. An axis for each of the three segments was identified from the RI: the shank axis was identified as the axis passing through the head of fibula and the lateral malleolus, the rearfoot axis was made to join the calcaneous to the fifth metatarsal head, the forefoot axis passed through the fifth metatarsal head and the toes (Fig. 2a). Moreover, in the RI, patches containing portions of the body segments, expected to show minimum changes in shape during movement, were identified (Fig. 2b). Axes and patches belonging to the same body segment were assumed to be rigidly connected.

2.5. Cross-correlation

Image cross-correlation was applied to the selected image patches to track the movement of the body segments. In image processing, cross-correlation is a well

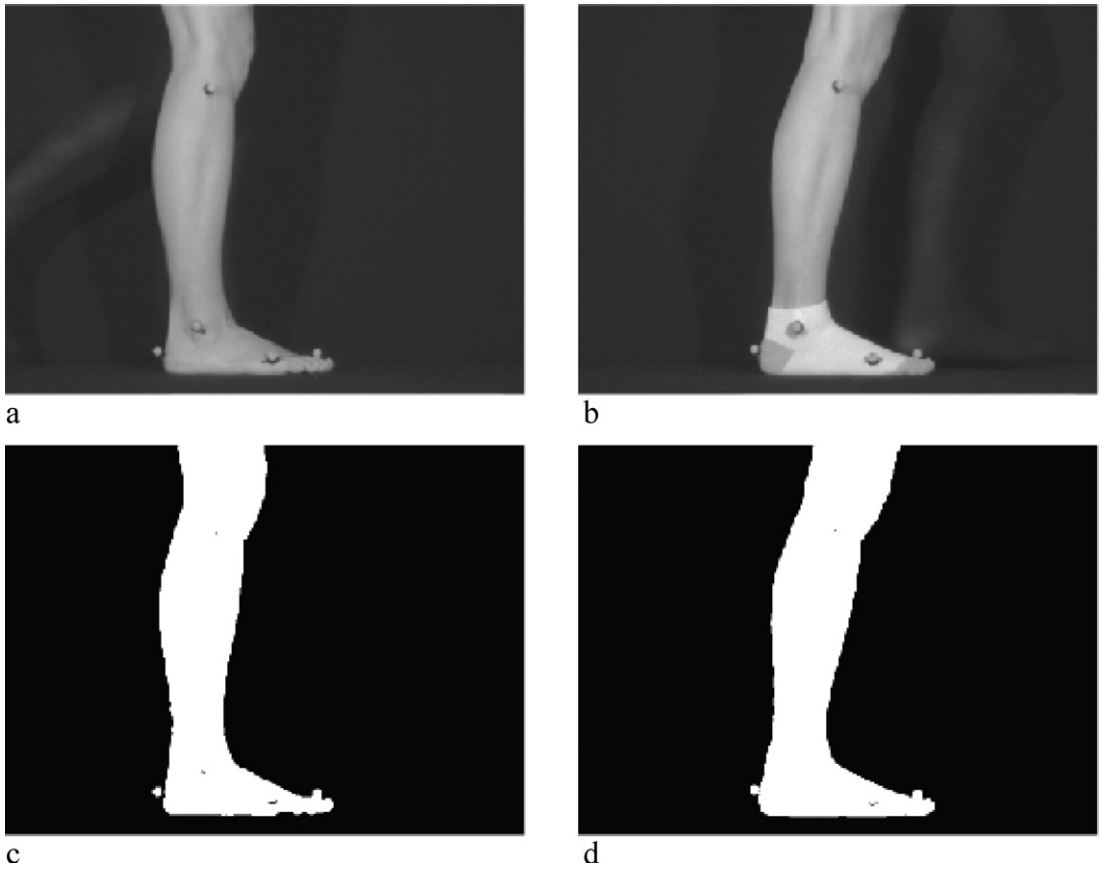

Fig. 1. Reference images of a subject barefoot (a) and wearing ankle socks (b). Relevant segmented output images (c and d).

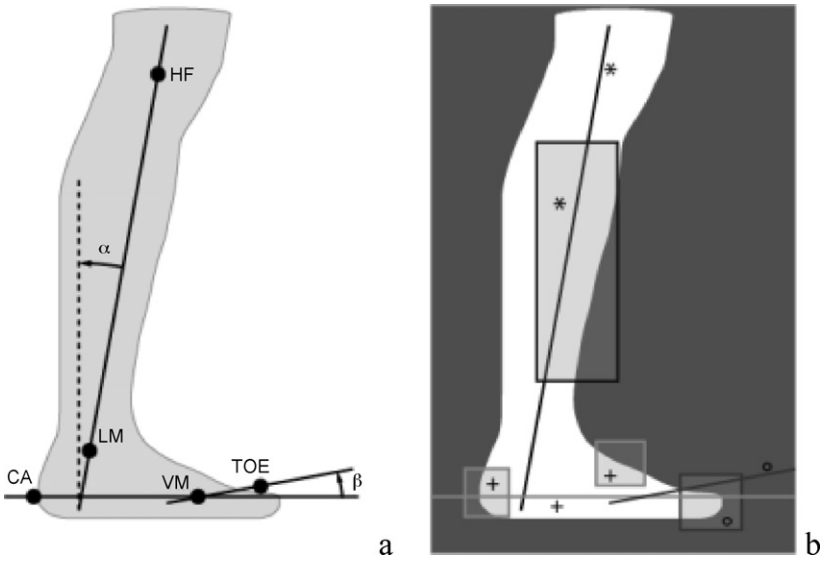

Fig. 2. Definition of ankle joint angle (α) and rearfoot–forefoot joint angle (β) (HF = head of fibula, LM = lateral malleolus, CA = calcaneus, VM = fifth metatarsal head, TOE = big toe) (a). Reference patches and anatomical axes (b). Symbols *, + and ◦ represent the anatomical axes and reference patches of shank, rearfoot and forefoot, respectively.

known and effective technique for template matching [17]. The cross-correlation coefficients, usually normalized in the range [0;1], express similarity between two different images: 1 represents full similarity, 0 no similarity.

The patches identified in the RI were searched in all the images of the sequence, one at the time, over a search space stemming from the possible translations and rotations. The patch in the searched image that showed the highest cross-correlation value was selected [18]. Cross-correlation coefficients were first computed translating the template along the vertical and horizontal axes of the whole picture. When a first maximum was found, then the patch was rotated by up to ten degrees and a second maximum was computed for each rotated patch over a limited search area. The highest cross-correlation value defined the position and orientation of the searched patch. The selected patch then became the new reference image for the succeeding frame and the whole procedure was repeated until the last frame.

2.6. Data analysis

The duration of the stance phase was defined as the number of the *MI* frames between heel strike and toe off. Since *MI* data and the *Mb* data were not synchronized, an *ad hoc* procedure was implemented. For each trial, heel-strike and toe-off event frames were selected. This was done through visual inspection on the *MI* frames and using force platform data for the *Mb* acquisitions. Since the *MI* frame rate was 1/8th of the *Mb* frame rate, the *Mb* frame best matching the *MI* event was defined as the *Mb* frame with α and β values most similar to the values obtained from the marker locations in *MI* event images.

Once the *MI* and *Mb* frames were aligned in time, the *Mb* sagittal joint kinematics were down-sampled to the *MI* frame rate for comparison purposes.

MI and *Mb* joint kinematics were compared as follows.

In order to account for offsets between the *MI* and the *Mb* ankle kinematics, the absolute difference between their mean values ($\overline{\alpha}_{MI}$ and $\overline{\alpha}_{Mb}$, respectively) over the stance phase was determined.

$$\Delta(\alpha) = |\overline{\alpha}_{MI} - \overline{\alpha}_{Mb}|$$

In order to account for pattern differences, for each time series the deviation from the mean values were determined:

$$\alpha'_{i\_MI} = \alpha_{i\_MI} - \overline{\alpha}_{MI}, \text{ and } \alpha'_{i\_Mb} = \alpha_{i\_Mb} - \overline{\alpha}_{Mb}$$

where the subscript i refers to the i^{th} frame; and the root mean square deviation (RMSD) of the α'_{i_MI} values from the α'_{i_Mb} values, was estimated:

$$\mathrm{RMSD}(\alpha'_{MI}, \alpha'_{Mb}) = \sqrt{\frac{\sum_{i=1}^{n} (\alpha'_{i\_MI} - \alpha'_{i\_Mb})^2}{n}}.$$

The same processing was applied to the rearfoot–forefoot joint kinematics (β).

To verify if measurements obtained with the two techniques were comparable to the intra-subject variability, similar indexes were introduced to estimate the intra-subject variability of the ankle kinematics obtained with the *Mb* measurements:

$$\Delta_V(\alpha) = |\overline{\alpha}_a - \overline{\alpha}_b| \text{ and}$$

$$\mathrm{RMSD}_V(\alpha'_a, \alpha'_b) = \sqrt{\frac{\sum_{i=1}^{n} (\alpha'_{i\_a} - \alpha'_{i\_b})^2}{n}},$$

where a and b represent any two of the five trials performed per condition per subject. Similar indexes were introduced for the β angle measurements.

The maximum values of $\Delta_V(\alpha)$ and $\mathrm{RMSD}_V(\alpha'_a, \alpha'_b)$ were compared to the maximum values of $\Delta(\alpha)$ and $\mathrm{RMSD}(\alpha'_{MI}, \alpha'_{Mb})$, and similarly was done for the indexes regarding the angle β.

3. Results

A representative sagittal joint kinematics during the stance phase, estimated with the *MI* technique and the *Mb* technique is reported in Fig. 3 for the three subjects.

The differences $\Delta(\alpha)$ and $\Delta(\beta)$ between the mean angle values for each trial and the maximum values of the intra-subject variability indexes $\Delta_V(\alpha)$ and $\Delta_V(\beta)$ are reported in Table 1. Table 2 shows the values of the RMSD of the joint angles α and β, $\mathrm{RMSD}(\alpha'_{MI}, \alpha'_{Mb})$ and $\mathrm{RMSD}(\beta'_{MI}, \beta'_{Mb})$, the maximum values of the intra-subject variability indexes $\mathrm{RMSD}_V(\alpha'_a, \alpha'_b)$ and $\mathrm{RMSD}_V(\beta'_a, \beta'_b)$ obtained for the three subjects in barefoot and socked conditions. No noticeable differences were found between barefoot and socked trials.

4. Discussion

3D marker-based motion capture systems are commonly used for estimating joint kinematics in clinical contexts. This approach requires expensive equipment and a high level of expertise to operate, limiting its use in clinical routine. Unfortunately, valid alternatives are not available yet. However, in some specific clinical issues, the determination of 2D joint kinematics is sufficient.

In this study, we presented a low-cost, low-discomfort markerless technique along with a preliminary validation and reliability assessment in estimating the sagittal kinematics of the shank and foot complex during the stance phase of normal walking.

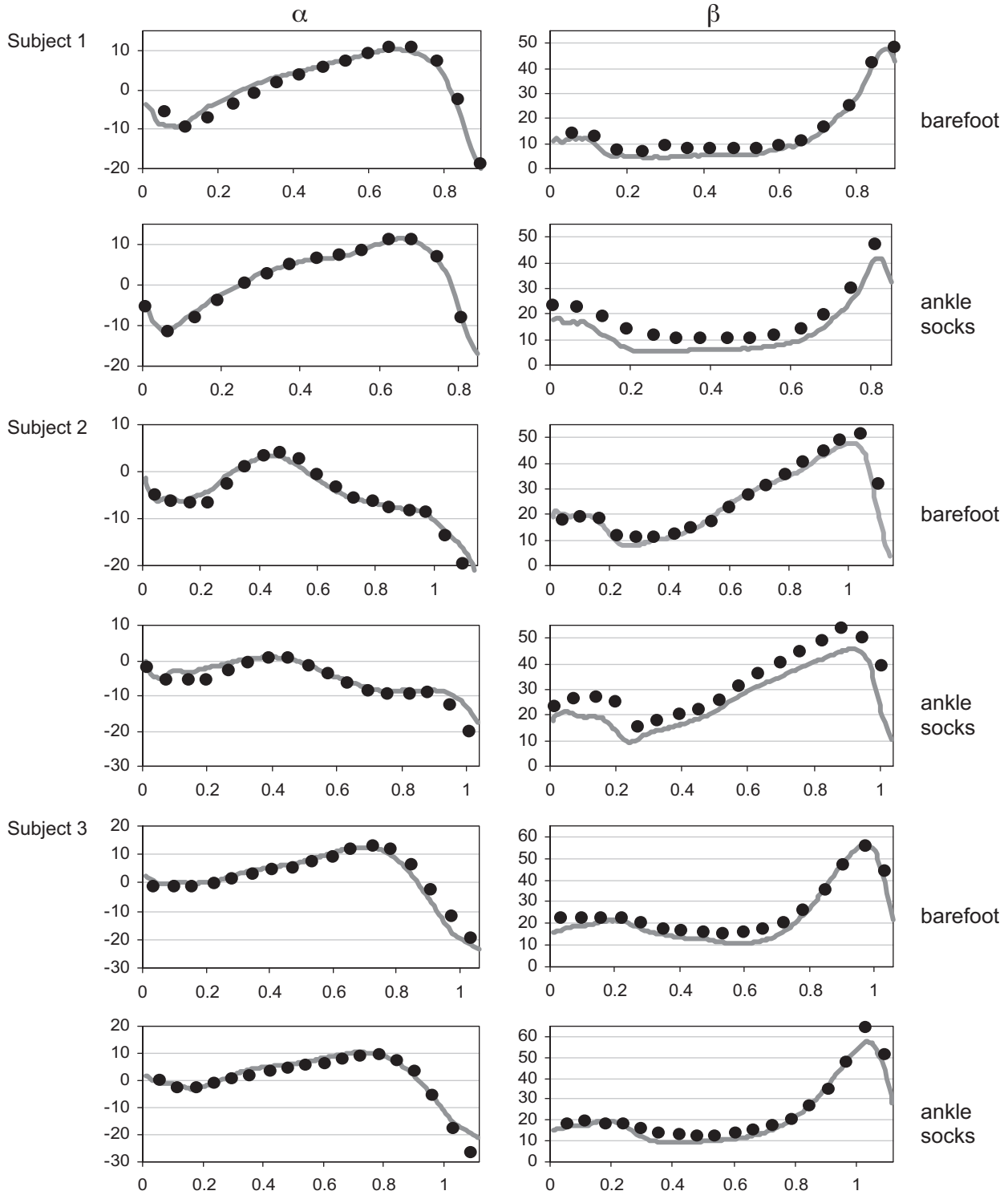

Fig. 3. Ankle kinematics (α) and rearfoot–forefoot joint kinematics (β) of three subjects (#1, #2, #3), obtained both in barefoot and socked conditions during the stance phase of walking. The solid lines are the joint kinematics obtained using the marker-based technique while dots are the joint kinematics obtained using the proposed markerless technique. Quantities are expressed in degrees.

The proposed technique requires a series of steps: video acquisition, segmentation, multi-rigid body model definition, anatomical axes definition and cross-correlation.

The segmentation outputs indicated that the algorithm chosen for segmenting the images had limited sensitivity to the presence of socks, suggesting that if subjects wore socks during the trials, results would not be affected. This can represent an advantage of the use of the *Ml* technique when analyzing the gait of subjects feeling more comfortable walking with socks than barefoot.

The ankle kinematics (α) estimated with the *Ml* and *Mb* techniques showed very similar results throughout the stance phase (both Δ and RMSD values are in general within the intra-subject variability). Differently, for the rearfoot–forefoot kinematics (β), Δ showed values about two degrees higher than the

Table 1
The absolute difference (Δ) between the mean values during stance of ankle (α) and rearfoot–forefoot (β) angles for each trial, condition and subject, obtained with marker-based and markerless techniques. Trial average and maximum values are also reported (in bold). In the grayed area the maximum intra-subject variability values (from marker-based measurements) of the absolute difference ($\Delta_{\mathbf{V}}$) are reported.

Angle (°)			Subject #1		Subject #2		Subject #3	
		Trial	Barefoot	Ankle socks	Barefoot	Ankle socks	Barefoot	Ankle socks
α	Δ	1	0.2	0.2	1.7	1.1	0.4	1
		2	0.2	0.7	2.5	0.8	0.2	0.6
		3	0.9	0.2	0.3	1.5	0.2	0.6
		4	1.5	0.8	0	2.2	1.1	1.4
		5	0	1.6	0	0.4	0.8	1.7
		Average	**0.6**	**0.7**	**0.9**	**1.2**	**0.6**	**1.0**
		Max	**1.5**	**1.6**	**2.5**	**2.2**	**1.1**	**1.7**
	Δ_V	*Max*	*2.5*	*3.3*	*1.6*	*1.9*	*2.1*	*1.8*
β	Δ	1	4.2	5.2	0.7	5.6	0.8	5.8
		2	2.4	3	6.9	8.2	2.4	3.1
		3	5.8	3.4	2.7	6	2.5	1.4
		4	5.4	3.2	0.6	6.9	1.5	4.2
		5	2.4	4.5	1.8	4.5	0.4	3.7
		Average	**4.0**	**3.9**	**2.5**	**6.2**	**1.5**	**3.6**
		Max	**5.8**	**5.2**	**6.9**	**8.2**	**2.5**	**5.8**
	Δ_V	*Max*	*2.9*	*2.5*	*5.9*	*6.5*	*4.4*	*3.4*

relevant intra-subject variability values (Δ_V) in all three subjects (except for the barefoot condition of subject #3). On the converse, the RMSD values for the β angle were in most cases within the relevant intra-subject variability index ($RMSD_V$). The different results obtained for the angle β are most probably due to the small size of the forefoot segment and consequently, to the lack of reliability in identifying the anatomical axis using either technique. The larger intra-subject variability determined for the angle β increases the chances of having larger differences in the joint kinematics estimated with the two techniques.

In general, the accuracy and precision of both *Ml* and *Mb* methods suffer from body segments of reduced size. *Mb* techniques perform better in identifying body segments orientation when segment markers are farther from each other (i.e. larger body segments). Similarly, *Ml* techniques may use a larger number of pixels to estimate the orientation of a large body segment. However, in general, while *Mb* techniques use a minimum number of points to describe the segment kinematics (typically three or four points), it is reasonable to expect that future *Ml* techniques may fruitfully use the redundancy of the information carried by the hundreds of pixels used to estimate the segment kinematics and may increase its precision. For instance, since markers are often located over a layer of soft tissues, near a joint or over an active muscle, their movement relatively to the underlying bone introduces errors in the estimation of joint kinematics [19,20]. The redundant number of points used by *Ml* techniques in determining segment kinematics could potentially reduce such errors.

5. Limitations and future work

The *Ml* technique employed in this study suffers of the same limitations of any 2D kinematics analysis of gait performed with a single camera. They are mostly related to the impossibility (a) of describing the out-of-plane joint kinematics, (b) of obtaining a bilateral analysis, (c) of describing segment deformity and (d) of keeping image plane and sagittal plane parallel. The last limitation has a limited effect on the resulting joint kinematics for small angles between the two mentioned planes (a 10° angle between planes generates a 1.5% difference in the sagittal joint kinematics estimate).

From an algorithmic standpoint, the chosen *Ml* technique shows limitations to be overcome for increasing its potential in clinical applications. To analyze the sagittal kinematics of pelvis

Table 2
Root mean square deviation (RMSD) estimated during stance of the markerless joint kinematics values from the marker-based joint kinematics (α and β) values. Trial average and maximum values are also reported (in bold). In the grayed area the maximum intra-subject variability values (from marker-based measurements) $RMSD_{\mathbf{V}}$ values are reported.

Angle (°)			Subject #1		Subject #2		Subject #3	
		Trial	Barefoot	Ankle socks	Barefoot	Ankle socks	Barefoot	Ankle socks
α	RMSD	1	1.6	0.6	1.7	1.6	3.4	1.7
		2	1.8	1.4	1.7	1.5	2.8	3
		3	2.6	0.7	2.1	1.3	2.4	2
		4	1.1	1.5	1.3	0.8	3.1	2.9
		5	0.7	2.7	1.1	2.4	2.7	2.2
		Average	**1.6**	**1.4**	**1.6**	**1.5**	**2.9**	**2.4**
		Max	**2.6**	**2.7**	**2.1**	**2.4**	**3.4**	**3**
	$RMSD_V$	*Max*	*4.1*	*2.7*	*2.8*	*3.0*	*2.6*	*4.2*
β	RMSD	1	2	1.2	2.8	4	5	2.3
		2	1.3	3.2	7.1	3.6	3	3.5
		3	3.7	1.7	3.7	5.1	2.3	2.6
		4	2.8	3.8	3.2	3.4	3.5	3.1
		5	1.6	3	3.8	3.4	3	2.7
		Average	**2.3**	**2.6**	**4.1**	**3.9**	**3.4**	**2.8**
		Max	**3.7**	**3.8**	**7.1**	**5.1**	**5**	**3.5**
	$RMSD_V$	*Max*	*3.2*	*3.9*	*6.6*	*6.5*	*3.1*	*6.5*

and lower limbs during the entire gait cycle, the improved *MI* technique should cope with complex backgrounds, shadows and occlusions. In this study, background subtraction was simplified by covering the contra-lateral leg with a long black sock. A more robust cross-correlation and/or image processing technique such as deformable contours [21] could help in solving the problem. Moreover, the processing time of the proposed *MI* technique in the current version implemented in MATLAB® (MathWorks, Natick, MA, USA) needs to be reduced to be fruitfully used in clinical applications (currently about 15 min are required to process a trial).

Finally, in order to assess the differences in the sagittal joint kinematics, the two techniques had to be registered at a reference point in time. This required the use of the markers located on anatomical landmarks for the definition of anatomical axes in the *MI* technique. As a consequence, this study does not provide information regarding the discrepancy (an offset) due to different ways of calibrating anatomical landmarks (from a reference image in a *MI* technique as opposed to palpation in a *Mb* technique). A reliable automatic anatomical axes identification procedure from the *MI* images would increase the robustness of the proposed technique.

6. Conclusion

The performance of the *MI* technique proposed to estimate 2D joint kinematics is promising for future use in clinical settings. In fact, the acquisition of movement data without the need of attaching markers to the subject's skin, and yet obtaining results comparable to those obtained with a simple marker based technique, represents an important step toward the design of an acquisition system for clinical use. Such a system could also be easy to configure and operate and most probably relatively affordable.

Acknowledgements

The authors thank the LabLab team coordinated by Prof. Aurelio Cappozzo (University of Rome "Foro Italico") for the help in setting up and carrying out the experimental work of this study.

Conflict of interest statement

There is no conflict of interest to be declared.

References

[1] Mündermann L, Corazza S, Andriacchi TP. The evolution of methods for the capture of human movement leading to markerless motion capture for bio-mechanical applications. Journal of NeuroEngineering and Rehabilitation 2006;3:6.
[2] Corazza S, Mündermann L, Chaudhari A, Demattio T, Cobelli C, Andriacchi TP. A markerless motion capture system to study musculoskeletal biomechanics: visual hull and simulated annealing approach. Annals of Biomedical Engineering 2006;34:1019–29.
[3] Bregler C, Malik J. Tracking people with twists and exponential maps. In: Proceedings of IEEE Computer Society Conference on Computer Vision and Pattern Recognition; 1998. p. 8–15.
[4] Chu CW, Jenkins OC, Matari MJ. Markerless kinematic model and motion capture from volume sequences. In: Proceedings of IEEE Computer Society Conference on Computer Vision and Pattern Recognition; 2003. p. 475–82.
[5] Azad P, Ude A, Asfour T, Cheng G, Dillmann R. Image-based markerless 3D human motion capture using multiple cues. In: Proceedings of the International Workshop on Vision Based Human-Robot Interaction; 2006.
[6] Deutscher J, Blake A, Reid I. Articulated body motion capture by annealed particle filtering. In: Proceedings of IEEE Computer Society Conference on Computer Vision and Pattern Recognition; 2000. p. 2126–33.
[7] Mundermann L, Corazza S, Chaudhari AM, Andriacchi TP, Sundaresan A, Chellappa R. Measuring human movement for biomechanical applications using markerless motion capture. In: Proceedings of SPIE – Three-dimensional image capture and applications VII; 2006. p. 1–10.
[8] Howe NR, Leventon ME, Freeman WT. Bayesian reconstruction of 3D human motion from single-camera video. In: Proceedings of Conference on Neural Information Processing System (NIPS) 12; 1999. p. 820–6.
[9] Poppe R. Vision-based human motion analysis: an overview. Computer Vision and Image Understanding 2007;108(1–2):4–18.
[10] Calhoun M, Longworth M, Chester VL. Gait patterns in children with autism. Clinical Biomechanics 2010.
[11] Picelli A, Camin M, Tinazzi M, Vangelista A, Cosentino A, Fiaschi A, et al. Three-dimensional motion analysis of the effects of auditory cueing on gait pattern in patients with Parkinson's disease: a preliminary investigation. Neurological Sciences 2010;31:423–30.
[12] Galli M, Cimolin V, Rigoldi C, Tenore N, Albertini G. Gait patterns in hemiplegic children with Cerebral Palsy: comparison of right and left hemiplegia. Research in Developmental Disabilities 2010;31:1340–5.
[13] Gage JR, DeLuca PA, Renshaw TS. Gait analysis: principles and applications: emphasis on its use in cerebral palsy. Journal of Bone and Joint Surgery 1995;77:1607–23.
[14] Chin R, Hsiao-Wecksler ET, Loth E, Kogler G, Manwaring SD, Tyson SN, et al. A pneumatic power harvesting ankle–foot orthosis to prevent foot-drop. Journal of Neuroengineering and Rehabilitation 2009;6:19.
[15] Stauffer C, Grimson WEL. Adaptive background mixture models for realtime tracking. In: Proceedings of IEEE Conference on Computer Vision and Pattern Recognition; 1999. p. 2246–52.
[16] Lagorio A, Grosso E, Tistarelli M. Automatic detection of adverse weather conditions in traffic scenes. In: Proceedings of 2008 IEEE International Conference on Advanced Video and Signal based Surveillance; 2008. p. 273–9.
[17] Goshtasby A, Gage SH, Bartholic JF. A two-stage cross-correlation approach to template matching. IEEE Transactions on Pattern Analysis and Machine Intelligence 1984;6:374–8.
[18] Lewis JP. Fast normalized cross-correlation. Vision Interface 1995;1:120–3.
[19] Cappozzo A, Catani F, Della Croce U, Leardini A. Position and orientation in space of bones during movement: anatomical frame definition and determination. Clinical Biomechnics 1995;10:171–8.
[20] Leardini A, Chiari L, Della Croce U, Cappozzo A. Human movement analysis using stereophotogrammetry: Part 3. Soft tissue artifact assessment and compensation. Gait & Posture 2005;21:212–25.
[21] Shahrokni A, Fleuret F, Fua P. Classifier-based contour tracking for rigid and deformable objects. In: Proceedings of the British Machine Vision Conference; 2005. p. 699–708.